frontiers | Frontiers in Materials

TYPE Original Research
PUBLISHED 05 December 2023
DOI 10.3389/fmats.2023.1334547

OPEN ACCESS

EDITED BY
Xiaolong Sun,
Guangdong University of Technology, China

REVIEWED BY
Fan Zhang,
Aalto University, Finland
Jinshun Xue,
Hubei University of Arts and Science, China

*CORRESPONDENCE
Keliang Mou,
2021021082@chd.edu.cn
Ting Zhang,
zhangt12@jlu.edu.cn

RECEIVED 07 November 2023
ACCEPTED 22 November 2023
PUBLISHED 05 December 2023

CITATION
Ji X, Mou K, Zhang T and Dong X (2023), Durability of geopolymer stabilized domestic waste incineration slag blending macadam in pavement base. *Front. Mater.* 10:1334547. doi: 10.3389/fmats.2023.1334547

Durability of geopolymer stabilized domestic waste incineration slag blending macadam in pavement base

Xiaoping Ji[1], Keliang Mou[1]*, Ting Zhang[2]* and Xinze Dong[3]

[1]School of Highway, Chang'an University, Xi'an, China, [2]School of Construction Engineering, Jilin University, Changchun, China, [3]Hefei Municipal Design and Research Institute Co Ltd., Hefei, China

In order to achieve the high quality and large-scale utilization of domestic waste incineration slag (WIS) in pavement base, a geopolymer prepared using fly ash from domestic waste incineration was used to replace the cement to stabilized WIS blending macadam used in the pavement base. The durability of the geopolymer stabilized WIS blending macadam (called as GeoWIS) was investigated, including the water stability, freeze-thaw resistance and dry shrinkage. The strength formation was identified using SEM analyses. Furthermore, the durability of GeoWIS was investigated and compared with those of cement stabilized macadam (CSM). Results show that the 7 days compressive strength of GeoWIS meets the strength criterion of the asphalt pavement base (≥2 MPa), except for the combination of 8% geopolymer and 100% WIS. The water stability coefficient and residual compressive strength ratio of GeoWIS increase as the geopolymer increases and WIS decreases. The cumulative dry shrinkage and dry shrinkage coefficient decrease as the WIS increases, while the cumulative water loss rate of GeoWIS increases. SEM analysis shows that the geopolymer reaction generates C-S-H gels, N-A-S-H gels, and Aft, which is the source of the GeoWIS strengths. GeoWIS has better water stability than CSM, and its freeze-thaw resistance and average dry shrinkage coefficient are lower than the average values for CSM.

KEYWORDS

road engineering, domestic waste incinerator slag, geopolymer, water stability, freeze-thaw resistance, dry shrinkage

1 Introduction

Due to the rapid urbanization, the worldwide production of domestic waste rapidly increase and has reached a huge scale (Long et al., 2021; Wang et al., 2022). Global domestic waste generation is currently 2.01 billion tons per year and is estimated to grow to 3.40 billion tons by 2050 (Zhang et al., 2021). The lack of timely disposal of domestic waste in cities causes environmental damage and spread diseases, which has seriously threatened the health of residents and hindered social development. In addition, some cities are facing the problem of "garbage siege" due to insufficient capacity to deal with domestic garbage. In response, many methods have been developed to deal with the domestic waste, such as landfilling, composting, and incineration (Huber et al., 2018; Wang et al., 2023). Incineration has become the main treatment technology for municipal domestic waste because of its energy recovery and capacity reduction features (Geng et al., 2020). However, incineration inevitably generates 5%–30% of domestic waste incineration slag (WIS), which is

hazardous by-products and needed further treatment (Ren et al., 2021). The rational disposal of WIS for reuse and recycling is gradually becoming a priority, both in terms of economic feasibility and environmental safety (Zhang et al., 2023; Zhang et al., 2024).

WIS is composed of fly ash and slag (Sarmiento et al., 2019). Fly ash refers to the residue collected from flue gas purification systems and heat recovery systems (such as heat exchangers, boilers, etc.), which contains harmful substances such as heavy metals and is classified as hazardous waste (Haiying et al., 2011; You et al., 2018). Slag is general solid waste, accounting for approximately 80% in WIS. The commonly fly ash disposal methods currently include cement solidification, chemical agent solidification, extraction and separation treatment, etc. These methods have their own advantages and limitations (Meijuan, 2016). The slag can be used for road engineering or brick making after being crushed and graded, but the current utilization rate is less than 50% (Kuo et al., 2015). On the other hand, road construction requires a large amount of cement and gravel materials, and using fly ash and slag for road construction is one of the effective ways to achieve large-scale reuse of WIS. The use of solid waste materials such as fly ash to prepare geopolymer instead of cement is the latest exploration direction for the high-value utilization of solid waste.

Geopolymer is a kind of inorganic binder obtained by dissolution-condensation reactions of silicate and aluminosilicate raw materials with alkali solutions (Hager et al., 2021). Fly ash from WIS is considered as a suitable raw material for the synthesis of geopolymer due to its silica-alumina phase and fine size. The silica-alumina phase of fly ash, as the determining factor of its activity, is insoluble in water and requires an alkali activator to boost (Xue et al., 2018). Many researches have chosen strong alkali activators such as NaOH, KOH or Na_2SiO_3 to break and release the active silica-alumina phase in fly ash (Çelikten et al., 2019). Yomthong et al. (2021) found that the compressive strength of fly ash-based geopolymer can reach 55.7 MPa, which was prepared with different molar ratios of Na_2SiO_3 and NaOH as alkali activator. The metakaolin, blast furnace slag, fiber and red mud are always added to further improve the performance of geopolymer (Liu et al., 2018; Li et al., 2019; Nuaklong et al., 2020; Faris et al., 2021; Chen et al., 2023). The addition of these materials can improve the Si/Al ratio, promote the polymerization reaction, and prolongs the initial setting time to a certain extent (Sinha et al., 2014). In addition, appropriate amount of fly ash mixed with cement can be used as a binder material, and the optimum ratio of fly ash to cement suitable for road base or subgrade was determined by studying its mechanical properties (Chompoorat et al., 2018; Liu et al., 2023). The results showed: the compressive strength of cement paste mixed with MSWI fly ash was reduced (Goh et al., 2003). Therefore, few researchers have used fly ash as a binder material for roads.

Recently, the WIS have been used in asphalt pavement base as an alternative to the natural aggregates. Yan et al. (2020) investigated the mechanical strength of cement stabilized natural macadam blending with WIS, and the results showed that the compressive strength meets the requirement of pavement base when the WIS replacement rate does not exceed 30%. Tian et al. (2016) prepared lime and fly ash co-stabilized natural macadam blending with WIS, and the results showed that the compressive strength is 1.25 MPa and exceeds the requirements of pavement base in "Specifications for Design of Highway Asphalt Pavement" when the WIS dosing does not exceed 50%. The above literature investigated the strength of the cement stabilized WIS, but the durability research is rarely reported.

The durability of asphalt pavement base refers to its ability to maintain structural durability under the continuous action of water, temperature and other factors, including water stability, freeze-thaw resistance and shrinkage resistance. Since the strength of WIS is lower than that of natural aggregate and contains more pores, the pavement base including WIS may cause a decline in material strength and micro-cracks after freeze-thaw or dry-wet cycles. Therefore, it is of great significance to study the durability of geopolymer stabilized WIS blending macadam.

In this research, fly ash from WIS was used to prepare geopolymer instead of cement to stabilize WIS blending macadam used in pavement base. The durability of geopolymer stabilized WIS blending macadam (GeoWIS) was evaluated, including water stability, freeze-thaw resistance and shrinkage property, and the effects of geopolymer dosing and WIS dosing on the durability were investigated. And also, the surface microstructure of GeoWIS was investigated by scanning electron microscopy (SEM) to explore the strength formation mechanism. Finally, the durability of GeoWIS was compared with cement stabilized macadam (CSM).

2 Materials and methods

2.1 Materials

2.1.1 Domestic waste incineration slag (WIS)

WIS was obtained from a domestic solid waste incineration plant, located in Xi'an, China. Its technical indicators were tested, presented in Table 1. The typical particle size of WIS was shown in Table 2. The morphology was observed by scanning electron microscopy (SEM) (Figure 1). WIS contains many substances formed by crystallization, and the surface is loose and porous.

2.1.2 Natural aggregates

The limestone was used in experiments and its technical indicators were presented in Table 3.

2.2 Fly ash-based geopolymer

Herein, the geopolymer was prepared from basic materials (fly ash and metakaolin) and alkali activators (i.e., NaOH and anhydrous sodium metasilicate). Fly ash was obtained from a domestic solid waste incineration plant, located in Xi'an, China. The chemical compositions were tested via XRF, and particle sizes were determined using a laser particle size analyzer. As shown in Table 4 and Figure 2, the main chemical components of fly ash are CaO, Na_2O, K_2O, and other types of oxides. The particles with a particle size <100 μm accounts for 93.64%, and the average particle size is 44.15 μm.

As the most basic active rock and soil mineral, SiO_2 and Al_2O_3 are the main substances for the polymerization reaction that leads to pozzolanic reaction with other alkaline materials to

TABLE 1 Technical index of WIS.

WIS	Apparent density (g/cm^3)	Flakiness content (%)	Crushed value (%)	Water absorption (%)
Coarse WIS	2.485	17.5	32.7	7.23
Fine WIS	2.205	-	-	9.26

TABLE 2 Particle size of WIS.

Material	Passing ratio (%) at different sieve sizes (mm)										
	19	16	13.2	9.5	4.75	2.36	1.18	0.6	0.3	0.15	0.075
Coarse WIS	100	98.1	95.6	84.6	18.1	2	0.5	0.3	0	0	0
Fine WIS	100	100	100	100	93.8	72.4	56.8	40.3	17.9	6.5	1.7

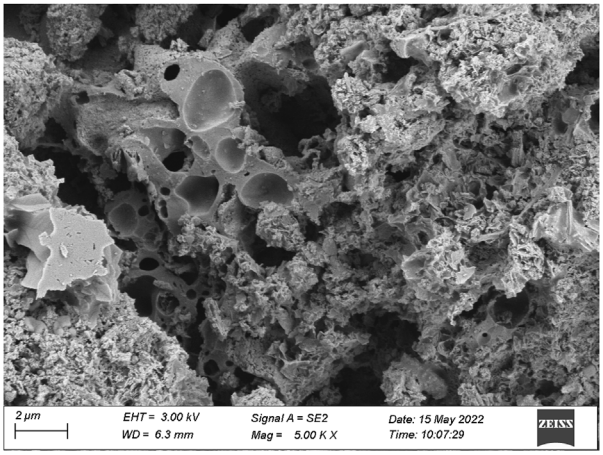

FIGURE 1
Scanning electron microscopy images of WIS.

produce strength. Owing to the low content of SiO_2 and Al_2O_3 in fly ash, materials including abundant SiO_2 and Al_2O_3 should be used to prepare geopolymers. Herein, metakaolin was selected, and the total content of SiO_2 and Al_2O_3 was 96.96% (Table 5). Figure 2 shows that the average particle size of the metakaolin is 33.2 μm.

In addition to these two materials, alkali activators are essential. Herein, NaOH and anhydrous sodium metasilicate were selected as alkali activators. The purity of NaOH is >96%, the aqueous solution anhydrous sodium metasilicate is alkaline for could supplying Na^+ and SiO_2. Figure 3 shows the main preparation process of the geopolymer.

The mass ratio of the prepared geopolymer was fly ash: metakaolin: NaOH: anhydrous sodium metasilicate: water = 0.10: 0.39:0.05:0.19:0.28. Table 6 presents the unconfined compressive strengths of the geopolymer cured at room temperature for 3 days, 7 days and 28 days. The results show that the 28 days unconfined compressive strength of the geopolymer is 29.58 MPa, which is close to that of cement (32.5 MPa).

2.3 Test methods

2.3.1 Unconfined compressive strength

The 7-day unconfined compressive strength of GeoWIS was carried out using an electronic universal material testing machine according to the "Test Methods of Materials Stabilized with Inorganic Binders for Highway Engineering" (JTG E51, 2009). Cylindrical specimens of size Φ150 mm × 150 mm were prepared, cured at room temperature for 6 days and were thereafter immersed in water for 24 h. The strain controlled loading rate was set as 0.5 mm/min. The unconfined compressive strength (R_c) of the specimen was calculate by Equation.

$$R_c = \frac{P}{A}$$

where R_c is the compressive strength (MPa); P is the maximum pressure when the specimen is damaged (N); A is the sectional area of specimen (mm^2).

Water stability

The GeoWIS specimens were soaked in water for 13 days after curing for 7 days, and then the compressive strength was tested, according to the Chinese Specification JTG E51-2009. The compressive strength was tested after soaking, and the water stability coefficient of the specimens was calculated as Equation.

$$K = \frac{R}{R_c}$$

where K is the water stability factor (%); R is the value of compressive strength of specimen after immersion for 13 days (MPa); R_c is the value of compressive strength of specimen (MPa).

2.3.2 Freeze-thaw

Cylindrical specimens of size Φ150 mm × 150 mm were prepared for the freeze-thaw. According to the Chinese Specification JTG E51-2009, the specimens were cured at room temperature for 6 days, soaked in water on the seventh day. Then, the specimen after immersion was alternately placed at −18 C for 16 h and in a water tank at 20 C for 8 h, which was one freeze-thaw cycle. The unconfined compressive strength of the specimen was

TABLE 3 Technical index of limestone.

item	Apparent density(g/cm^3)	Flakiness content(%)	Crushed value(%)
19–31.5	2.732	11.5	-
9.5–19	2.719	8.4	17.7
Specification	-	≤20	≤30

TABLE 4 Chemical compositions of fly ash.

Component	CaO	Cl	Na_2O	K_2O	SO_3	SiO_2	MgO	Al_2O_3	ZnO	Fe_2O_3
Content (%)	33.98	30.85	15.73	9.08	4.22	2.26	1.40	0.735	0.549	0.485

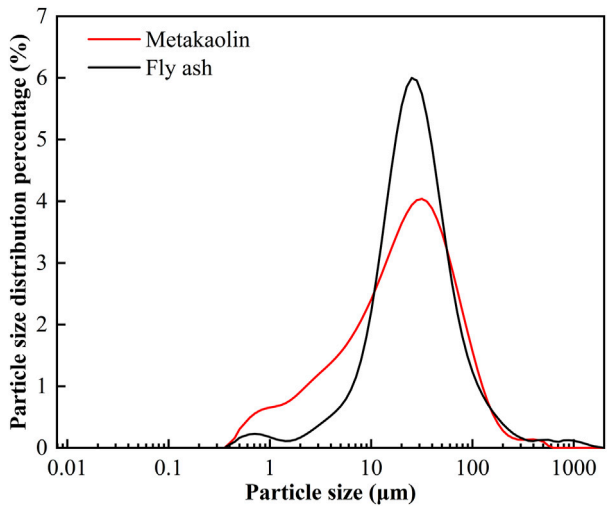

FIGURE 2
Particle size of fly ash and metakaolin.

tested after five freeze-thaw cycles. The freeze resistance index of specimen was calculated as Equation.

$$BDR = \frac{R_{DC}}{R_C} \times 100$$

where BDR is the residual strength ratio (%); R_{DC} is the compressive strength of the specimen after 5 freeze-thaw cycles (MPa); R_C is the compressive strength of the specimen (MPa).

2.3.3 Dry shrinkage

The dry shrinkage of GeoWIS was performed in a drying oven with a constant temperature of 20°C ± 1°C and a relative humidity of 60% ± 5%, according to the Chinese Specification (JTG E51, 2009). Beam specimens of 100 mm × 100 mm × 400 mm were used for dry shrinkage. The initial length and mass of the specimen were measured after 7 days of curing at room temperature. Then the dial indicator was fixed on the dry shrinkage apparatus, and the dial indicator was connected with the specimen of the sample. The specimen and the shrinkage apparatus were put into the drying chamber together. The corresponding dial indicator reading and the mass of each specimen was recorded once a day in the first week of the test and once 2 days from the second week, the test period was set as 30 days. The water loss rate, dry shrinkage, dry shrinkage strain and dry shrinkage coefficient of the mixture specimen were calculated according to Equaiton.

TABLE 6 Results of the unconfined compressive strength of geopolymer (MPa).

Curing (d)	3d	7d	28d
Compressive strength (MPa)	27.95	29.16	29.58

$$\omega_i = \frac{m_i - m_{i-1}}{m_p} \times 100$$

$$\delta_i = \sum_{j-1}^{2} X_{i,j} - \sum_{j-1}^{2} X_{i+1,j}$$

$$\varepsilon_i = \frac{\delta_i}{l}$$

$$\alpha_{di} = \frac{\varepsilon_i}{\omega_i}$$

where ω_i is water loss rate of the specimen (%); i is the days of the specimens placed in a dry environment (i = 1,2. . .); m_i is the measurement quality of the standard specimen (g); m_p is the mass of standard specimen after drying (g); δ_i is the dry shrinkage of the specimen (mm); $X_{i,j}$ is the readings of dial indicators (mm); j represents different dial indicators (j = 1,2. . .); ε_i is the dry shrinkage strain (%); α_{di} is the dry shrinkage coefficient (%); l is the standard specimen length (mm).

3 Methodology

Considering the large density difference between WIS and limestone, WIS with a particle size of 0–9.5 mm was selected to

TABLE 5 Chemical composition of metakaolin.

Component	SiO_2	Al_2O_3	TiO_2	Fe_2O_3	CaO	K_2O	MgO	ZrO_2	P_2O_5	Na_2O
Content (%)	54.06	42.90	1.25	0.559	0.334	0.197	0.196	0.130	0.0845	0.0699

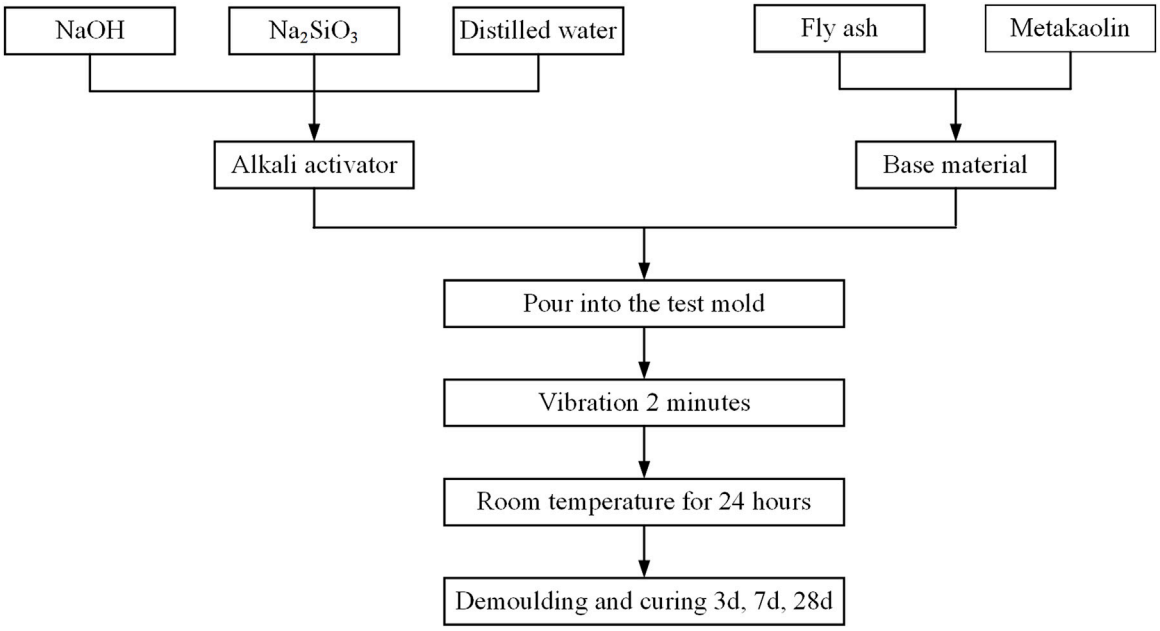

FIGURE 3
Fly ash-based geopolymer preparation.

TABLE 7 Gradation of GeoWIS.

Particle size (mm)	Mass percentage of 0% WIS content (%)		Mass percentage of 50% WIS content (%)		Mass percentage of 100% WIS content (%)		Upper limit	Lower limit
	WIS	Macadam	WIS	Macadam	WIS	Macadam		
31.5	0	20.60	0	21.50	0	22.48	100	100
19.0	0	33.14	0	34.58	0	36.16	86	68
9.5	0	17.24	7.27	9.00	15.20	0	58	38
4.75	0	9.47	4.08	4.94	8.54	0	32	22
2.36	0	8.18	3.52	4.27	7.37	0	28	16
0.6	0	9.08	3.91	4.74	8.18	0	15	8
0.075	0	2.29	0.99	1.20	2.07	0	3	0

TABLE 8 Test scheme.

Items	Curing condition	Mass percentage of geopolymer content (%)	Mass percentage of WIS content (%)
Unconfined compressive strength	Curing at room temperature for 6 d and soaking in water for 24 h	8, 10, 12, 14	0, 50, 100
Water stability	7 d at room temperature followed by 13 d of water immersion	8, 10, 12	0, 50
		10, 12, 14	100
Freeze-thaw	6 d at room temperature followed by water immersion on day 7th	8, 10, 12	0, 50
		10, 12, 14	100
Dry shrinkage	Curing at room temperature for 7 d	12	0, 50, 100

10.3389/fmats.2023.1334547

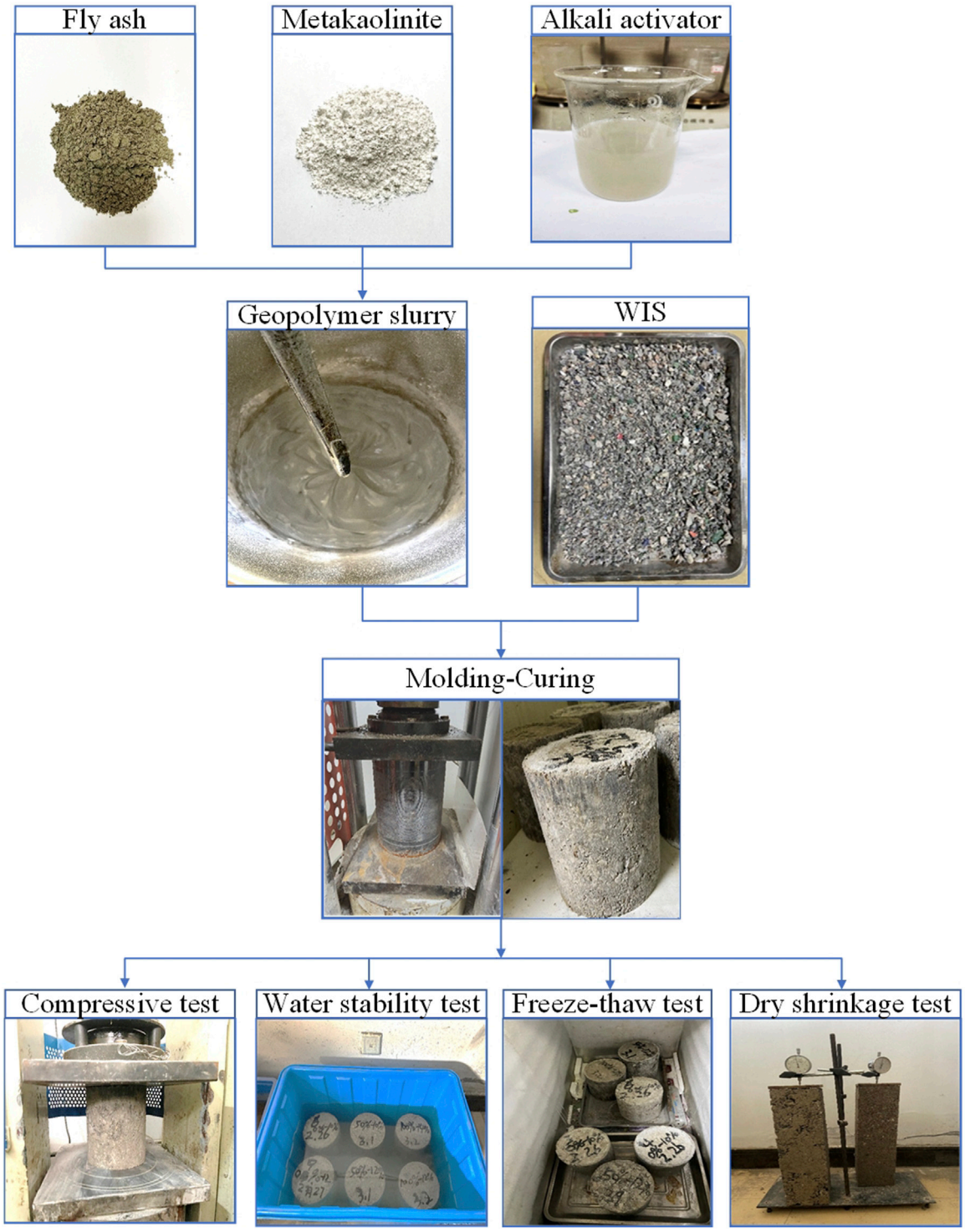

FIGURE 4
Experimental procedure.

replace limestone in equal volume to form a skeleton-dense structure. The initially selected replacement levels for WIS were 0%, 50%, and 100%. Table 7 presents the mixture design with different mass percentages of WIS substituting limestone.

In this study, GeoWIS was prepared by varying the amount of the geopolymer and WIS doping, and its 7 days unconfined compressive strength, water stability, freeze–thaw, and dry shrinkage were tested. Table 8 shows the test scheme, where the geopolymer content is the mass ratio of aggregate. Figure 4 presents the corresponding test procedure.

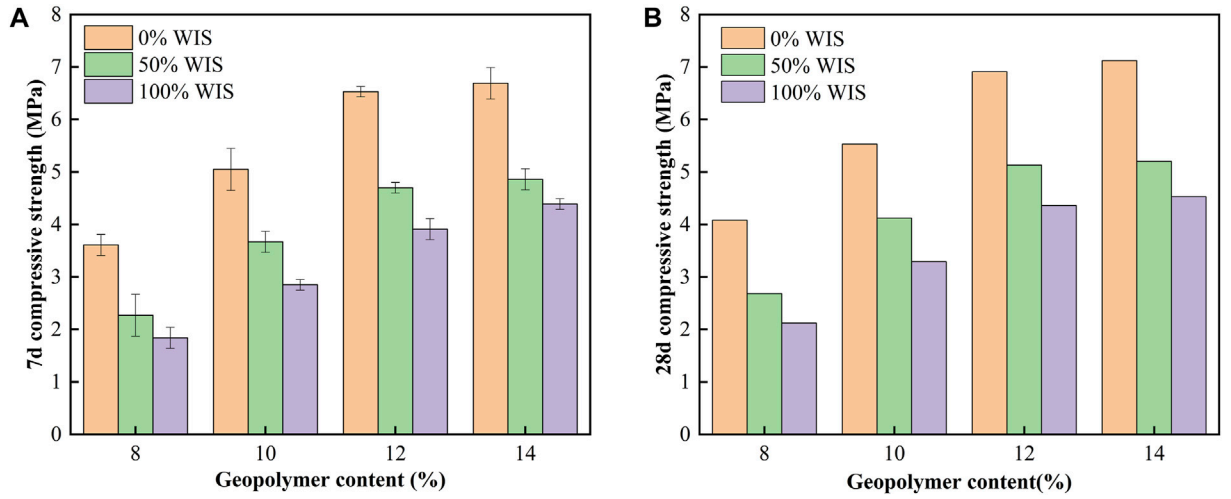

FIGURE 5
(A) 7-days compressive strength of GeoWIS, **(B)** 28-days compressive strength of GeoWIS.

TABLE 9 Reqirement of 7-day unconfined compressive strength for cement stabilized materials.

Structural layers	Highway classification	Very heavy traffic (MPa)	Heavy traffic (MPa)	Medium and light traffic (MPa)
Base layer	Expressways and first-class highways	5.0–7.0	4.0–6.0	3.0–5.0
	Secondary and sub-secondary highways	4.0–6.0	3.0–5.0	2.0–4.0
Subbase layer	Expressways and first-class highways	3.0–5.0	2.5–4.5	2.0–4.0
	Secondary and sub-secondary highways	2.5–4.5	2.0–4.0	1.0–3.0

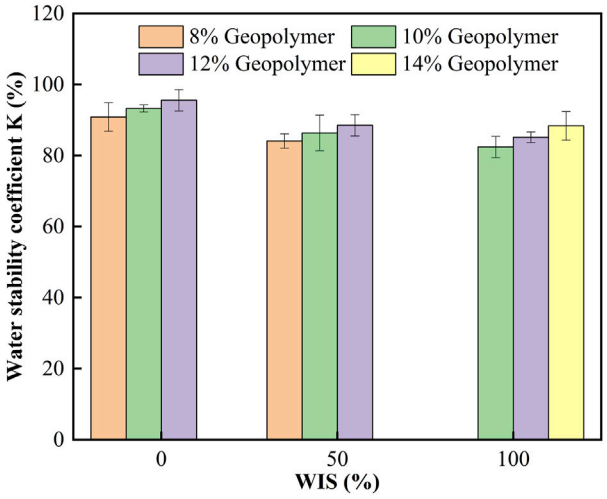

FIGURE 6
Water stability of GeoWIS.

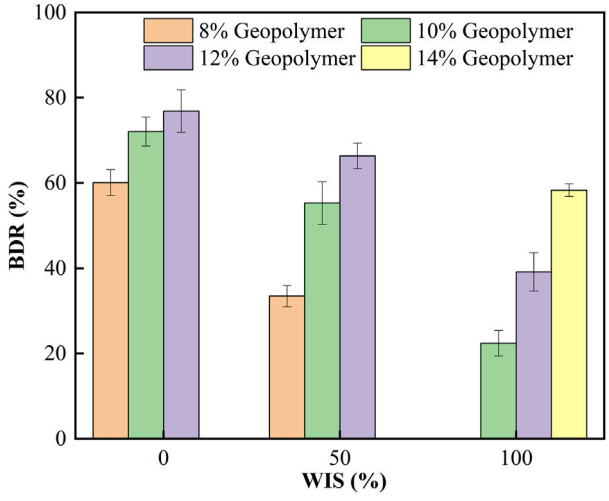

FIGURE 7
Freeze-thaw resistance of GeoWIS.

4 Results and discussions

4.1 Unconfined compressive strength

Figure 5A illustrated the results of the 7 days unconfined compressive strength of GeoWIS. The compressive strength of GeoWIS with different WIS content increases as the geopolymer content increases, which is resulted from that the C-S-H and N-A-S-H cementitious materials in the mixture increase with the increase of geopolymer content. The C-S-H and N-A-S-H cementitious

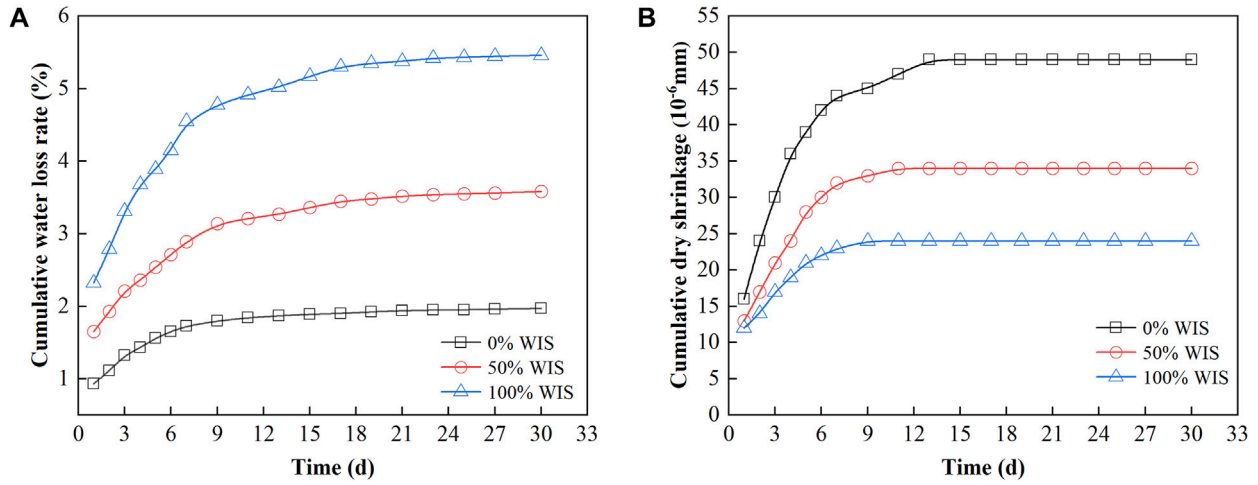

FIGURE 8
Accumulative water loss rate vs. accumulative dry shrinkage. **(A)** Accumulative water loss rate; **(B)** Accumulative dry shrinkage.

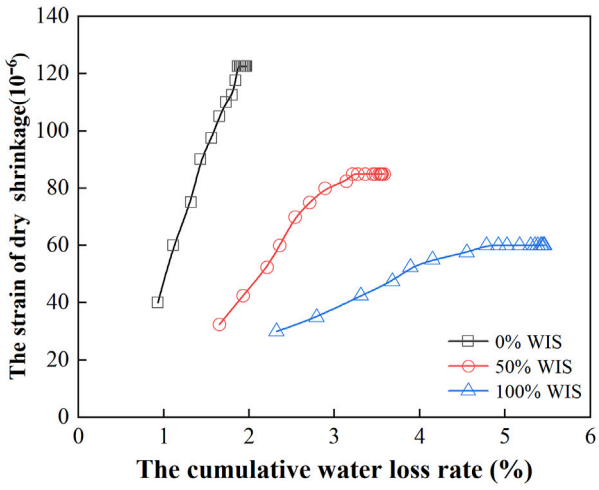

FIGURE 9
Dry shrinkage strain vs. accumulative water loss rate.

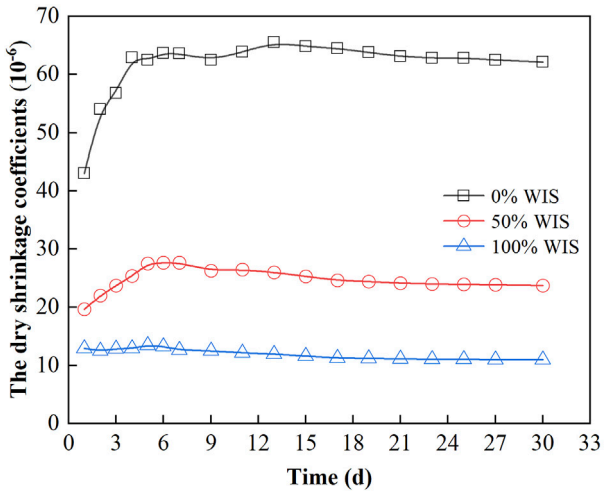

FIGURE 10
Dry shrinkage coefficient vs. time.

materials not only fill the pores in the mixture, but also enhance the cementation with the aggregate and form a dense structure. However, the compressive strength of GeoWIS with the same geopolymer content decreases as the WIS content increases. The compressive strength of GeoWIS is 1.84 MPa when the WIS content is 100% and the geopolymer content is 8%, which was lower than the minimum strength standard required by the specification. This is due to the fact that the strength of WIS is lower than that of limestone aggregates. The substitution of WIS for limestone creates a weak zone within the specimen that is detrimental to the strength of GeoWIS. Figure 5B showed the 28-day unconfined compressive strength of GeoWIS, and the strength trend is generally consistent with that of the 7-day. Therefore, in the subsequent study, the geopolymer content of 8% was not used when the WIS content was 100%.

Further analysis revealed that the geopolymer stabilized macadam meets the strength requirements of any highway and traffic classification for base and subbase when the geopolymer content exceeds 10%. (Table 9).

4.2 Water stability

Figure 6 showed the results of water stability test. The water stability coefficient of GeoWIS increases with the increase of geopolymer content at the same WIS content, and the water stability coefficients of all mixtures are over 83%. When the content of WIS increases, the water stability coefficient of GeoWIS decreases under the same geopolymer content. This is attributed to the fact that WIS has greater porosity and water absorption than limestone

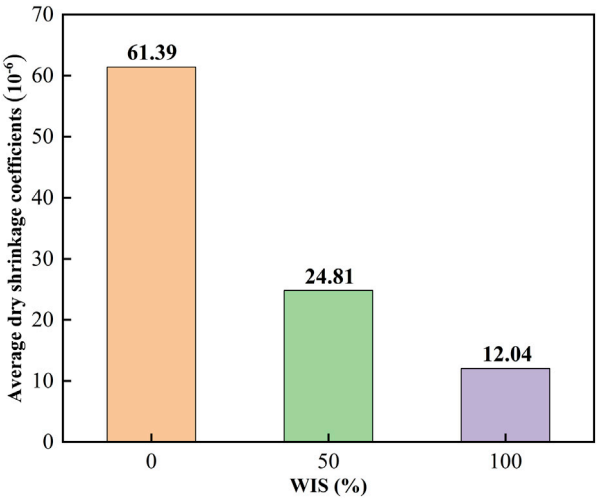

FIGURE 11
Average shrinkage coefficient vs. WIS content.

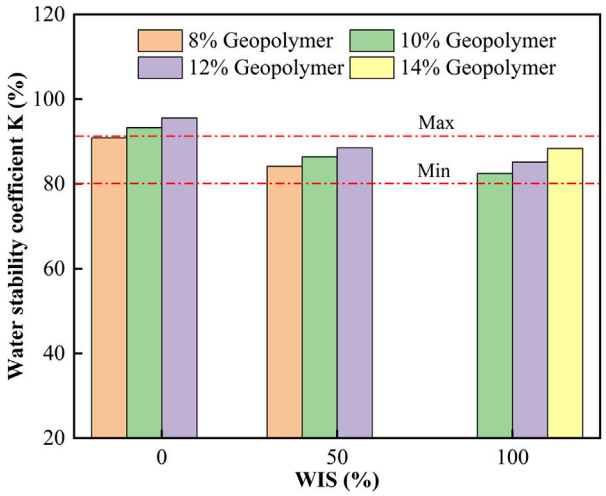

FIGURE 13
Comparison of water stability of GeoWIS with CSM.

aggregate. More pores and pore walls in the mixture become softened and permeated by water as WIS content rises. This causes a significant amount of water to enter the specimen interior, which in turn weakens the internal bonding force and structural stability of the specimen and reduces GeoWIS strength.

4.3 Freeze-thaw resistance

The freeze-thaw performance was shown in Figure 7. The BDR of GeoWIS increases as the geopolymer increases and WIS decreases after 5 freeze-thaw cycles. The reason for this is that as the geopolymer content increases, the increased C-S-H and N-A-S-H cementitious materials in the mixture enhance the bond strength to the aggregate, while effectively preventing the development and expansion of internal pores, and the freeze-thaw resistance of GeoWIS is enhanced. However, the high water absorption and porosity of WIS can lead to water filled pores and cracks when the specimens are immersed, and the water expands in volume after freezing to further open the pores causing severe damage to the specimens. In addition, the high substitution rate of WIS leads to a reduction in the strength of GeoWIS and the specimens are more susceptible to damage by water expansion. As a result, the BDR of GeoWIS decreases with increasing WIS content after freeze-thaw cycles.

4.4 Dry shrinkage property

The proportion of WIS instead of limestone is unchanged, and 12% geopolymer was selected to study the change of dry

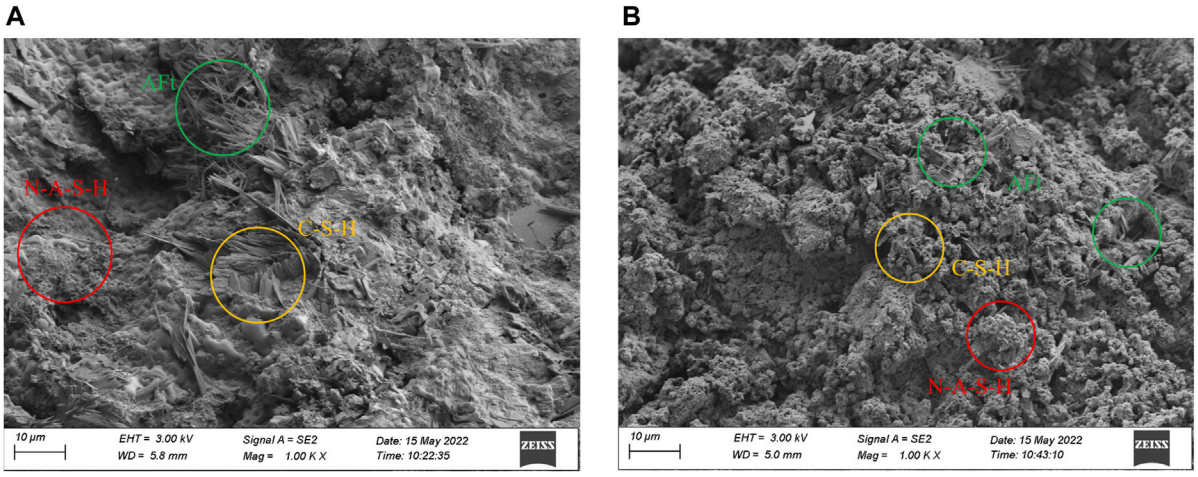

FIGURE 12
SEM picture of macadam and GeoWIS. **(A)** Macadam; **(B)** WIS.

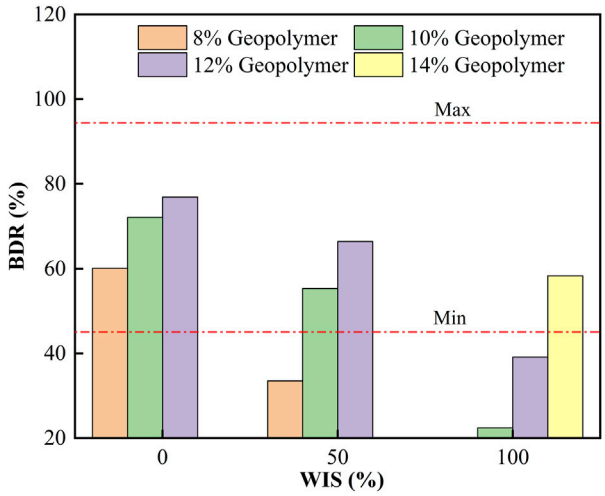

FIGURE 14
Comparison of freeze-thaw resistance of GeoWIS with CSM.

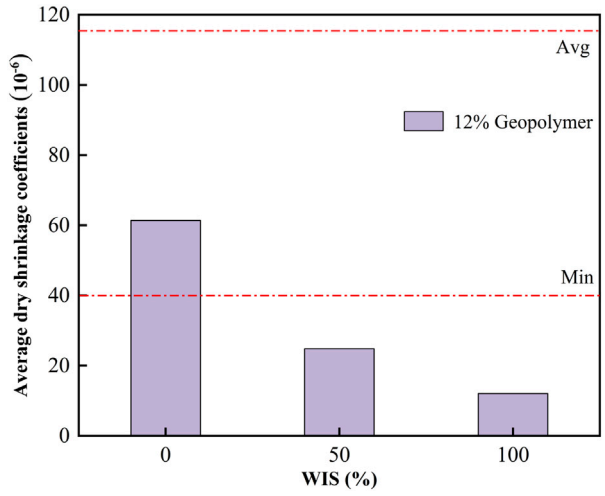

FIGURE 15
Comparison of dry shrinkage coefficients of GeoWIS with CSM.

shrinkage performance of GeoWIS. The dry shrinkage test results were shown in Figure 8, Figure 9, Figure 10, Figure 11. Figure 8A illustrated the curve of the cumulative water loss rate with time. The cumulative water loss rate of the three mixtures all shows an increasing trend with the increase of time, after 9 days, the increasing trend of cumulative water loss rate tends to be flat. The cumulative water loss rate increases with the increase of WIS content for the same curing time, which is caused by the higher water content of WIS than limestone. The water loss rate and water content are positively correlated, and the higher the WIS content, the greater the cumulative water loss rate. Figure 8B showed the relationship between dry shrinkage strain and time. The cumulative dry shrinkage strain of the three mixes increases first and then becomes flat as time increases. The cumulative shrinkage strain decreases significantly with increasing WIS content. The density of WIS is less than that of limestone aggregate, which decreases the weight of the specimens when the substitution rate of WIS increases. The geopolymer content is fixed and the shrinkage sources C-S-H gel and N-A-S-H gel are reduced by decreasing the geopolymer content in the specimens. Therefore, increasing the WIS content helps to improve the cumulative shrinkage strain of GeoWIS.

The change curve of dry shrinkage strain against cumulative water loss rate was shown in Figure 9. The dry shrinkage strain of the three mixtures gradually increases while the slope gradually decreases with the increase in cumulative water loss. The higher the WIS content, the lower the dry shrinkage strain of GeoWIS. At the same dry shrinkage strain, the cumulative water loss of GeoWIS increases with the increase of WIS content. The water loss of the specimens includes C-S-H gel, N-A-S-H gel, capillary adsorbed water and free water in macropores, among which free water in macropores has less effect on the dry shrinkage strain, while the adsorbed water evaporated in capillary pore and cementitious materials dehydrated have more effect on the dry shrinkage strain (Yang et al., 2019). Since WIS instead of limestone aggregate will increase the macropores free water of the mixture, and the first evaporation of the macropore free water has little effect on the dry shrinkage of the mixture, the slope of the curve decreases with the increase of WIS content.

The change of dry shrinkage coefficients with time were shown in Figure 10. The dry shrinkage coefficients gradually increase with the increase of observation time, and basically enter the plateau after 9 days. The dry shrinkage coefficients of the mixture with WIS content are significantly smaller than that of the mixture without WIS. The dry shrinkage coefficients of the mixture with 100% WIS content tend to be flat on the overall and hold the minimum value.

Figure 11 showed the average dry shrinkage coefficients of GeoWIS. The average dry shrinkage coefficient drops significantly with the increase of WIS content, with the lowest value occurring after the complete replacement of limestone by WIS. This is because the free water loss contained in WIS does not affect the drying shrinkage. In a word, the dry shrinkage resistance of GeoWIS without WIS incorporation is weak, but its dry shrinkage resistance can be significantly improved by adding WIS content.

4.5 SEM analysis

The SEM pictures of GeoWIS surfaces were displayed in Figure 12. It can be seen that lumpy, and irregular substances C-S-H, rod-shaped or needle-shaped Aft, and flocculent N-A-S-H can be observed in hydrated products of GeoWIS. The AFt microcrystals can fill the pores and make the structure more compact. The byproducts of polymerization reactions, C-S-H and N-A-S-H, can bind particles together to boost aggregate strength (Sinha et al., 2014; Ji et al., 2023). The C-S-H, N-A-S-H, and Aft generated by the polymerization reaction change the microstructure and pores of the aggregate, forming a dense and strong matrix. It is worth noting that the WIS surface contains more voids (black) than the gravel surface, which explains why the strength of the sample decreases with the increase of the WIS substitution rate.

TABLE 10 Durability statistics of CSM.

Resources	Water stability coefficient (%)	Freeze-thaw resistance (%)	Dry shrinkage coefficient (10^{-6})	Mixture properties
Cao (2004)	86.0	45.0	40.0	Basalt, 32.5 cement, 4.0% cement content
Huang (2022)	91.0	-	126.0	Limestone, 42.5 cement, 5.0% cement content
Du et al. (2019)	80.0	88.0	-	Sandstone, 32.5 cement, 3.5% cement content
Liu (2021)	87.9	-	-	Limestone, 32.5 cement, 4.0% cement content
Chu et al. (2022)	87.4	-	-	Limestone, 42.5 cement, 4.0% cement content
Zhang et al. (2023)	-	75.9	-	Andesite, 32.5 cement, 6% cement content
Guan et al. (2021)	-	94.3	-	Coal gangue, 42.5 cement, 5.0% cement content
Fan (2022)		93.07		Limestone, 42.5 cement, 5.0% cement content
Xu (2022)	-	88.0	-	Limestone, 42.5 cement, 4.0% cement content
Zhang (2020)	-	80.4	-	Iron tailings, 32.5 cement, 8.0% cement content
Shen et al. (2021)	-	-	96.4	Limestone, 32.5 cement, 3.0% cement content
Li et al. (2021)	-	-	58.3	Limestone, 42.5 cement, 3.5% cement content
Yan et al. (2020)	-	-	140.0	Limestone, 32.5 cement, 4.5% cement content
Yan et al. (2019)	-	-	238.6	Limestone, 32.5 cement, 5% cement content
Statistical result	Max: 91.0	Max: 94.3	Max: 238.6	-
	Min: 80.0	Min: 45.0	Min: 40.0	
	Avg: 86.5	Avg: 80.7	Avg: 116.5	

4.6 Comparison between GeoWIS and cement stabilized macadam

To better understand the durability performance of GeoWIS, the water stability, freeze-thaw resistance, and dry shrinkage coefficient of GeoWIS and cement stabilized macadam (CSM) were investigated, respectively, and the results were shown in Figure 13, Figure 14, Figure 15 and Table 10. According to the comparison in Figure 13, Figure 14, Figure 15, the water stability of GeoWIS is close to that of CSM, the freeze-thaw resistance is lower than that of CSM, and the dry shrinkage resistance is better than that of CSM.

The durability statistics of CSM were shown in Table 10. It can be seen from Table 6 that the overall water stability of GeoWIS is at least 2.5% higher than the minimum value of water stability of CSM. The BDR values of GeoWIS are all lower than the average value of BDR of CSM by at least 1.7%. The average dry shrinkage coefficient of GeoWIS is at least 55.1% lower than the average value of average dry shrinkage coefficient of CSM.

5 Conclusion

(1) When the content of geopolymer exceeds 10%, the geopolymer stabilized macadam meets the strength requirements of the base and subbase of any highway and traffic classification. When the polymer content is 8%, in addition to do not meet the heavy traffic expressway base and subbase, and expressway heavy traffic base requirements, other requirements.

(2) The overall water stability of GeoWIS is at least 2.5% higher than the minimum value of water stability of CSM. All of the BDR values for GeoWIS are at least 1.7% less than the average BDR value for CSM. The average dry shrinkage coefficient of GeoWIS is at least 55.1% lower than the average value of average dry shrinkage coefficient of CSM.

(3) Corresponding to different highway classifications, expressways and first-class highways can use 50% WIS content instead of natural aggregates for all traffic classes except very heavy traffic, while secondary and sub-secondary

highways can use 100% content instead of natural aggregates for all traffic classifications.

Data availability statement

The original contributions presented in the study are included in the article/Supplementary material, further inquiries can be directed to the corresponding authors.

Author contributions

XJ: Conceptualization, Funding acquisition, Supervision, Writing–review and editing. KM: Formal Analysis, Writing–original draft. TZ: Supervision, Writing–review and editing. XD: Formal Analysis, Investigation, Methodology, Writing–original draft.

Funding

The author(s) declare financial support was received for the research, authorship, and/or publication of this article. This work was supported by the Key R&D Plan of Shaanxi Province (2023-YBSF-390), Transportation Technology Project of Shaanxi Province (23-97k), and Scientific Research Fund of Xinjiang Transportation Design Institute (KY2022080901, KY2022042501).

Conflict of interest

Author XD was employed by Hefei Municipal Design and Research Institute Co Ltd.

The remaining authors declare that the research was conducted in the absence of any commercial or financial relationships that could be construed as a potential conflict of interest.

Publisher's note

References

Cao, X. (2004). Research on application of municipal solid waste combustion residues for freeway pavement base. Master Thesis. Nanjing, China: Nanjing University of Aeronautics and Astronautics.

Çelikten, S., Sarıdemir, M., and Deneme, İ. Ö. (2019). Mechanical and microstructural properties of alkali-activated slag and slag+ fly ash mortars exposed to high temperature. *Constr. Build. Mater.* 217, 50–61. doi:10.1016/j.conbuildmat.2019.05.055

Chen, Y., Ji, X., Si, B., Zhang, Z., Shao, D., Zhu, S., et al. (2023). Investigation on self-healing performance of asphalt mixture containing microcapsules and survival behaviour of microcapsules. *Int. J. Pavement Eng.* 24 (1), 2165657. doi:10.1080/10298436.2023.2165657

Chompoorat, T., Likitlersuang, S., and Jongvivatsakul, P. (2018). The performance of controlled low-strength material base supporting a high-volume asphalt pavement. *KSCE J. Civ. Eng.* 22 (6), 2055–2063. doi:10.1007/s12205-018-1527-z

Chu, F., Sun, J., Wang, R., Ji, P., Wang, X., and Liu, J. (2022). Study on influence of performance of cement stabilized macadam mixture with iron tailings sand. *J. Wuhan Univ. Technol.* 2022, 1–7.

Du, Q., Pan, T., Lv, J., Zhou, J., Ma, Q., and Sun, Q. (2019). Mechanical properties of sandstone cement-stabilized macadam. *Appl. Sci.* 9 (17), 3460. doi:10.3390/app9173460

Fan, W. (2022). Study on frost resistance of micro-crack cement stabilized gravel base material. *Heilongjiang Transp. Technol.* 45, 55. doi:10.16402/j.cnki.issn1008-3383.2022.01.036

Faris, M. A., Tahir, M. F. M., Hashim, M. F. A., Samad, A. A., Ramasamy, S., and Nawi, M. A.-H. M. (2021). *The improvement of fly ash based geopolymer concrete by inclusion of hooked steel fibers*. Arau, Malaysia: AIP Publishing LLC, 020246.

Geng, C., Liu, J., Wu, S., Jia, Y., Du, B., and Yu, S. (2020). Novel method for comprehensive utilization of MSWI fly ash through co-reduction with red mud to prepare crude alloy and cleaned slag. *J. Hazard. Mater.* 384, 121315. doi:10.1016/j.jhazmat.2019.121315

Goh, C.-C., Show, K.-Y., and Cheong, H.-K. (2003). Municipal solid waste fly ash as a blended cement material. *J. Mater. Civ. Eng.* 15 (6), 513–523. doi:10.1061/(asce)0899-1561(2003)15:6(513)

Guan, J., Lu, M., Yao, X., Wang, Q., Wang, D., Yang, B., et al. (2021). An experimental study of the road performance of cement stabilized coal gangue. *Crystals* 11 (8), 993. doi:10.3390/cryst11080993

Hager, I., Sitarz, M., and Mróz, K. (2021). Fly-ash based geopolymer mortar for high-temperature application–Effect of slag addition. *J. Clean. Prod.* 316, 128168. doi:10.1016/j.jclepro.2021.128168

Haiying, Z., Youcai, Z., and Jingyu, Q. (2011). Utilization of municipal solid waste incineration (MSWI) fly ash in ceramic brick: product characterization and environmental toxicity. *Waste Manag.* 31 (2), 331–341. doi:10.1016/j.wasman.2010.10.017

Huang, T. (2022). Study on the performance of cement stabilized bottom ash pellets/macadam mixture. Master Thesis. Yanzhou, China: Yangzhou University.

Huber, F., Laner, D., and Fellner, J. (2018). Comparative life cycle assessment of MSWI fly ash treatment and disposal. *Waste Manag.* 73, 392–403. doi:10.1016/j.wasman.2017.06.004

Ji, X., Chen, B., Dong, X., Lu, H., Zhang, X., He, S., et al. (2023). Mechanical and environmental properties of geopolymer-stabilized domestic waste incineration slag in an asphalt pavement base. *J. Road Eng.* 3 (2), 218–228. doi:10.1016/j.jreng.2023.04.001

JTG E51 (2009). *Test methods of materials stabilized with inorganic binders for highway engineering*. Beijing: China Communications Press.

Kuo, W.-T., Liu, C.-C., and Shu, C.-Y. (2015). The feasibility of using washed municipal solid waste incinerator bottom ash in compressed mortar paving units. *J. Mar. Sci. Technol.* 23 (3), 13. doi:10.6119/JMST-014-0416-7

Li, Q., Gao, P., Wang, Y., Zhao, H., and Liu, J. (2021). Study on drying shrinkage and crack resistance of cement (fly ash) stabilized coal gasification porous slag. *J. China Foreign Highw.* 2, 288. doi:10.14048/j.issn.1671-2579.2021.05.061

Li, Y., Min, X., Ke, Y., Liu, D., and Tang, C. (2019). Preparation of red mud-based geopolymer materials from MSWI fly ash and red mud by mechanical activation. *Waste Manag.* 83, 202–208. doi:10.1016/j.wasman.2018.11.019

Liu, J., Wang, B., Hu, C. T., Chen, J. G., Zhu, S. Y., and Xu, X. D. (2023). Multiscale study of the road performance of cement and fly ash stabilized aeolian sand gravel base. *Constr. Build. Mater.* 397, 131842. doi:10.1016/j.conbuildmat.2023.131842

Liu, N. (2021). Research on road performance of coal gangue in cement stabilized crushed stone base. Master Thesis. Yinchuan, China: Ningxia University.

Liu, X., Zhao, X., Yin, H., Chen, J., and Zhang, N. (2018). Intermediate-calcium based cementitious materials prepared by MSWI fly ash and other solid wastes: hydration characteristics and heavy metals solidification behavior. *J. Hazard. Mater.* 349, 262–271. doi:10.1016/j.jhazmat.2017.12.072

Long, W.-J., Peng, J.-K., Gu, Y.-C., Li, J.-L., Dong, B., Xing, F., et al. (2021). Recycled use of municipal solid waste incinerator fly ash and ferronickel slag for eco-friendly mortar through geopolymer technology. *J. Clean. Prod.* 307, 127281. doi:10.1016/j.jclepro.2021.127281

Meijuan, J. (2016). Study on technoloy of solidification of municipal solid wastes incineration (MSWI) fly ash by cement. *Chin. J. Environ. Eng.* 10 (6), 3235–3241.

Nuaklong, P., Jongvivatsakul, P., Pothisiri, T., Sata, V., and Chindaprasirt, P. (2020). Influence of rice husk ash on mechanical properties and fire resistance of recycled aggregate high-calcium fly ash geopolymer concrete. *J. Clean. Prod.* 252, 119797. doi:10.1016/j.jclepro.2019.119797

Ren, J., Hu, L., Dong, Z., Tang, L., Xing, F., and Liu, J. (2021). Effect of silica fume on the mechanical property and hydration characteristic of alkali-activated municipal solid waste incinerator (MSWI) fly ash. *J. Clean. Prod.* 295, 126317. doi:10.1016/j.jclepro.2021.126317

Sarmiento, L. M., Clavier, K. A., Paris, J. M., Ferraro, C. C., and Townsend, T. G. (2019). Critical examination of recycled municipal solid waste incineration ash as a mineral source for portland cement manufacture – a case study. *Resour. Conservation Recycl.* 148, 1–10. doi:10.1016/j.resconrec.2019.05.002

Shen, Y., Wang, Z., Ye, S., and Qiu, S. (2021). Research on dry shrinkage performance of cement stabilized macadam with dense skeleton. *Beifang Jiaotong* 2021 (03), 67–69+73. doi:10.15996/j.cnki.bfjt.2021.03.017

Sinha, D. K., Kumar, A., and Kumar, S. (2014). Development of geopolymer concrete from fly ash and bottom ash mixture. *Trans. Indian Ceram. Soc.* 73 (2), 143–148. doi:10.1080/0371750x.2014.922427

Tian, M., Ma, G., Yong, L., Dong, W., Tao, Z., and Meng, L. (2016). Application study of municipal solid waste incineration slag in road material. *Energy Conservation Environ. Prot.* 2016, 1.

Wang, C., Li, Y., Wen, P., Zeng, W., and Wang, X. (2022). A comprehensive review on mechanical properties of green controlled low strength materials. *Constr. Build. Mater.* 363, 129611. doi:10.1016/j.conbuildmat.2022.129611

Wang, S., Wang, C., Yuan, H., Ji, X., Yu, G., and Jia, X. (2023). Size effect of piezoelectric energy harvester for road with high efficiency electrical properties. *Appl. Energy* 330, 120379. doi:10.1016/j.apenergy.2022.120379

Xu, X. (2022). Damage characteristics and numerical simulation analysis of cement-stabilized macadam base in season frozen regions. Master Thesis. Changchun, China: Jilin University.

Xue, X., Liu, Y.-L., Dai, J.-G., Poon, C.-S., Zhang, W.-D., and Zhang, P. (2018). Inhibiting efflorescence formation on fly ash–based geopolymer via silane surface modification. *Cem. Concr. Compos.* 94, 43–52. doi:10.1016/j.cemconcomp.2018.08.013

Yan, K., Gao, F., Sun, H., Ge, D., and Yang, S. (2019). Effects of municipal solid waste incineration fly ash on the characterization of cement-stabilized macadam. *Constr. Build. Mater.* 207, 181–189. doi:10.1016/j.conbuildmat.2019.02.048

Yan, K., Sun, H., Gao, F., Ge, D., and You, L. (2020). Assessment and mechanism analysis of municipal solid waste incineration bottom ash as aggregate in cement stabilized macadam. *J. Clean. Prod.* 244 (20), 118750. doi:10.1016/j.jclepro.2019.118750

Yang, J., Liu, L., Liao, Q., Wu, J., Li, J., and Zhang, L. (2019). Effect of superabsorbent polymers on the drying and autogenous shrinkage properties of self-leveling mortar. *Constr. Build. Mater.* 201, 401–407. doi:10.1016/j.conbuildmat.2018.12.197

Yomthong, K., Wattanasiriwech, D., Aungkavattana, P., and Wattanasiriwech, S. (2021). Effect of NaOH concentration and curing regimes on compressive strength of fly ash-based geopolymer. *Mater. Today Proc.* 43, 2647–2654. doi:10.1016/j.matpr.2020.04.630

You, L., You, Z., Yang, X., Ge, D., and Lv, S. (2018). Laboratory testing of rheological behavior of water-foamed bitumen. *J. Mater. Civ. Eng.* 30 (8), 04018153. doi:10.1061/(asce)mt.1943-5533.0002362

Zhang, F., Sha, A., Cao, Y., Wang, W., and Song, R. (2024). Microwave heating moment, thermal characteristics, and structural variations of different steel slag asphalt mixtures suffered from freeze-thaw damage. *Cold Regions Sci. Technol.* 217, 104028. doi:10.1016/j.coldregions.2023.104028

Zhang, F., Sha, A., Cao, Y., Wang, W., Song, R., and Jiao, W. (2023). Characterization of self-healing properties of asphalt pavement materials containing carbon nanotubes: from the binder and mix level based on grey relational analysis. *Constr. Build. Mater.* 404, 133323. doi:10.1016/j.conbuildmat.2023.133323

Zhang, J. (2020). Experimental study on road durability of curing agent stabilized iron tailing. MSc thesis. China: Hebei University of Architecture.

Zhang, Y., Wang, L., Chen, L., Ma, B., Zhang, Y., Ni, W., et al. (2021). Treatment of municipal solid waste incineration fly ash: state-of-the-art technologies and future perspectives. *J. Hazard. Mater.* 411, 125132. doi:10.1016/j.jhazmat.2021.125132